Available online at www.sciencedirect.com
SCIENCE DIRECT®
Coordination Chemistry Reviews 249 (2005) 1372–1381
COORDINATION CHEMISTRY REVIEWS
www.elsevier.com/locate/ccr

Review

Photophysics of supramolecular binary stacks consisting of electron-rich trinuclear Au(I) complexes and organic electrophiles

Mohammad A. Omary [a,**], Ahmed A. Mohamed [b], Manal A. Rawashdeh-Omary [a], John P. Fackler Jr. [b,*]

[a] *Department of Chemistry, University of North Texas, P.O. Box 305070, Denton, TX 76203, USA*
[b] *Department of Chemistry, Texas A&M University, P.O. Box 30012, College Station, TX 77843, USA*

Received 2 August 2004; accepted 10 December 2004
Available online 28 March 2005

Contents

Abstract

Two nucleophilic trinuclear Au(I) ring complexes, $Au_3((p\text{-tolyl})N=C(OEt))_3$, **1**, and $Au_3(\mu\text{-}C^2,N^3\text{-bzim})_3$, **2**, form sandwich adducts with organic Lewis acids (C_6F_6 and $C_{10}F_8$) and electron acceptors (tetracyanoquinodimethane, TCNQ), a neutral polyfunctional inorganic Lewis acid ($Hg_3(o\text{-}C_6F_4)_3$), and naked heavy metal cations (Tl^+ and Ag^+). Fascinating photophysical properties are associated with the adducts formed, including external heavy-atom effect leading to room-temperature phosphorescence of aromatic molecules, quenching of luminescence upon exposure to organic vapors, and sensitization of metal-centered emissions in supramolecular stacks with luminescence thermochromism. Intermolecular interactions, including M–M bonding and π acid–base interactions, play the major role in influencing the luminescence properties.

Keywords: Trinuclear Au(I) complexes; Phosphorescence; Heavy-atom effect; Aurophilic bonding; X-ray structures

1. Introduction

The Lewis donor–acceptor concept [1] and the related Ingold–Robinson nucleophile–electrophile concept [2] are traditionally associated with σ donation and acceptance

* Corresponding author. Tel.: +1 979 845 0648; fax: +1 979 845 2373.
** Co-corresponding author.
E-mail addresses: mo0029@unt.edu (M.A. Omary), fackler@mail.chem.tamu.edu (J.P. Fackler Jr.).

0010-8545/$ – see front matter © 2005 Elsevier B.V. All rights reserved.
doi:10.1016/j.ccr.2004.12.018

of "electron pairs" [3]. But with the development of organometallic chemistry, it has become critical to expand these concepts to include π acids and bases. Conventionally, the π base is an unsaturated organic molecule while metal centers are usually acids/acceptors. Our recent efforts, however, have demonstrated that the trinuclear Au(I) compounds with substituted imidazolate and carbeniate bridging ligands, Plate 1, act as π bases which form supramolecular stacks with a variety of electrophiles [4–8]. These electrophiles include organic Lewis acids (C_6F_6 and $C_{10}F_8$) and electron acceptors (tetracyanoquinodimethane, TCNQ), a neutral polyfunctional inorganic Lewis acid ($Hg_3(o\text{-}C_6F_4)_3$), and naked heavy metal cations (Tl^+ and Ag^+). The resulting sandwich adducts exhibit interesting bonding and optoelectronic properties. The focus of this article is photophysical properties of the trinuclear Au(I) complexes and the sandwich π adducts thereof with organic electrophiles. A review of the structural properties of trinuclear Au(I) complexes in general has been reported elsewhere [9].

Our efforts are complementary to those by others in areas that span structural, chemical, and physical properties of extended-chain materials and trinuclear d^{10} ring complexes. Extended linear-chain compounds that contain metal atoms exhibit important aspects in chemical bonding as well as fascinating chemical and physical properties [10–12]. Many classes of coordination compounds that exhibit such structures have been reported, giving rise to advances in several areas that include supramolecular architecture, acid–base chemistry, metallophilic bonding, luminescent materials, optical sensing, and various optoelectronic applications. Among the many recent developments in this area are reports about a vapochromic light-emitting diode from linear-chain Pt(II)/Pd(II) complexes [13], a luminescent switch consisting of an Au(I) dithiocarbamate complex that possesses a luminescent linear chain in the presence of vapors of organic solvents [14], a vapochromic complex, $\{Tl[Au(C_6Cl_5)_2]\}_n$, that shows a quantum dot effect and reversible color changes upon binding to volatile organics [15], a modified form of Magnus' green salt $[(NH_3)_4Pt][PtCl_4]$, that exhibits semiconducting properties [16], a variety of d^8 complexes that interact with inorganic [17] and organic [18] molecules to form donor–acceptor extended-chain adducts with interesting conducting and/or magnetic properties, and new interesting complexes that exhibit strong heterobimetallic bonding between different closed-shell metal ions [19,20].

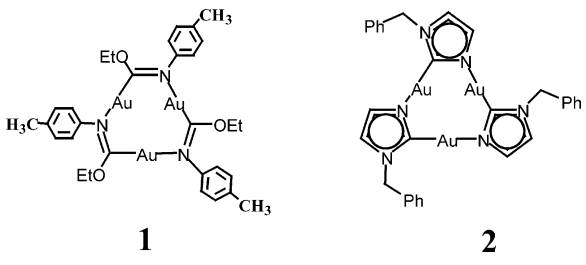

Plate 1. Sketch of the trinuclear Au^I compounds studied.

An especially intriguing class of linear-chain species involves trinuclear d^{10} complexes, which have garnered considerable interest in recent years owing in large part to their fascinating luminescence properties. For example, Balch and co-workers reported that a trinuclear carbeniate Au(I) complex exhibits "solvoluminescence", i.e., it produces spontaneous orange emission upon contact with solvent in samples that had been irradiated with long-wavelength UV light [21a]. The same and related complexes have been found to form charge-transfer complexes with nitro-9-fluorenones [21b] and some form hourglass figures on standing or when placed in an acid [21c]. The combined work reported by us [7], Balch and co-workers [21], and Yang and Raptis [22] indicates that the luminescence of the trinuclear Au(I) complexes, regardless of the bridging ligand, is related to intermolecular Au–Au interactions between adjacent trimers. Gabbaï and co-workers have reported that a trinuclear Hg(II) complex forms 1:1 adducts with aromatic hydrocarbons, which become brightly phosphorescent at room temperature due to a mercury heavy-atom effect [23,24]. Finally, a recent report by Dias et al. showed that a trinuclear Cu(I) pyrazolate complex exhibits bright emissions that can be tuned to multiple luminescence colors across the visible region by varying the temperature, solvent, or concentration [25].

2. Isolated trinuclear compounds

2.1. Nucleophilic nature

The two trinuclear Au(I) ring complexes that we have focused on, $Au_3((p\text{-tolyl})N{=}C(OEt))_3$, **1**, and $Au_3(\mu\text{-}C^2,N^3\text{-}bzim)_3$, **2**, are shown in Plate 1. The two compounds stack as dimers in the solid state with a chair arrangement in **1** [26] and a prismatic arrangement in **2** [27]. Hence, each compound exhibits both intramolecular and intermolecular Au–Au interactions, i.e., *aurophilic bonding* [28]. Density-functional theory calculations have indicated that **1** and **2** are electron-rich species. Two views are shown in Fig. 1 to illustrate the negative molecular electrostatic potential (MEP); the positive and negative MEP regions in space are shown for the crystallographic arrangement of **1** while the MEP values are mapped on the electron density surface of **2** [7]. The most nucleophilic regions are clearly at the center of the trinuclear ring and they extend in the space perpendicular to the ring plane. Hence, the π base concept for **1** and **2** is borne out according to the data in Fig. 1. This is similar to the action of aromatic hydrocarbons as π bases that can attract cations at the center of and perpendicular to the aromatic ring plane; see the work of Dougherty on cation-π interactions [29]. In fact, **1** and **2** are involved in strong cation-π interactions, as they form sandwich adducts with Tl^+ and Ag^+ ions, which have been fully characterized by X-ray crystallography and exhibit fascinating luminescence properties [4,5]. Such adducts are not discussed in detail in this review, however, as the major focus herein is on the trinuclear species alone and their adducts with organic electrophiles.

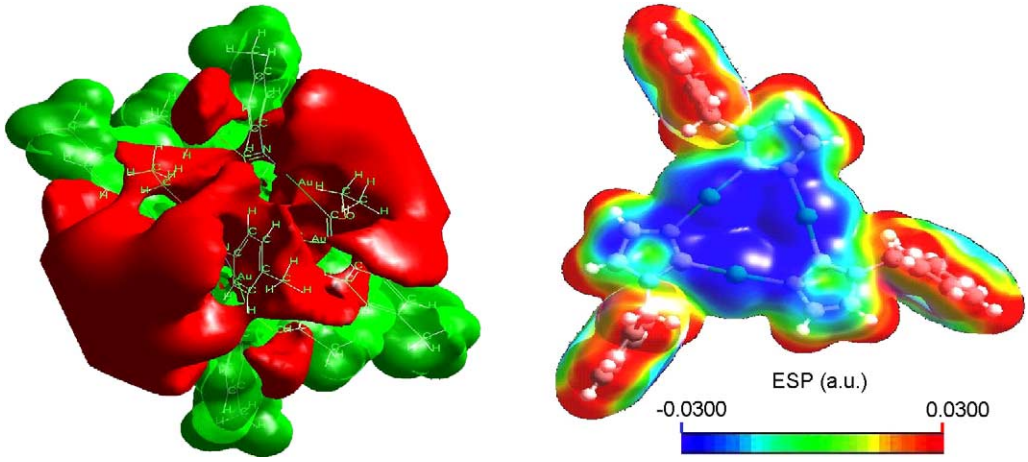

Fig. 1. Representation of the molecular electrostatic potential (MEP) from DFT calculations [7]. The positive (green) and negative (red) MEP regions in space are shown for the crystallographic arrangement of a dimeric unit of **1** (left) while the MEP values are mapped on the electron density surface of a molecule of **2** (right).

2.2. Photophysics

The luminescence emission and excitation spectra of **1** in the solid state are shown in Fig. 2. The solid exhibits a feeble blue luminescence that becomes bright at 77 K. The lifetime is ~10 μs [30], hence the emission is phosphorescence from a formally triplet excited state. The emission shows a structured profile with a uniform vibronic spacing (~1400 cm^{-1}). This spacing corresponds to the Raman spectrum of **1** in solution, which shows a peak at ~1422 cm^{-1} and an overtone thereof (Fig. 3, right). This peak is assignable to the ν_{C-N} vibration of the bridging carbeniate ligand. The higher frequency region shows other vibrations characteristic of the aliphatic and aromatic substituents in **1** on the blue and red side of 3000 cm^{-1}, respectively. At first sight, it is tempting to assign the blue emission of **1** to a ligand-centered phosphorescence from a single molecular unit of **1**. This is because the emission is highly structured, typical of ligand-centered emissions in monomeric organic molecules/ligands and because the vibronic spacing corresponds to the ν_{C-N} vibration in a dilute solution. However, further data in Section 3.2 below suggest that the emission likely occurs from a dimeric unit. Furthermore, the luminescence excitation spectra show peaks at too low energies to be assigned to a monomeric species. The emitting state, therefore, is likely a ligand to metal–metal charge transfer (LMMCT).

3. Adducts with organic electrophiles

3.1. Perfluoronaphthalene adduct

Reaction of **1** with octafluoronaphthalene, $C_{10}F_8$, forms a bright yellow phosphorescent solid [31]. The crystal structure

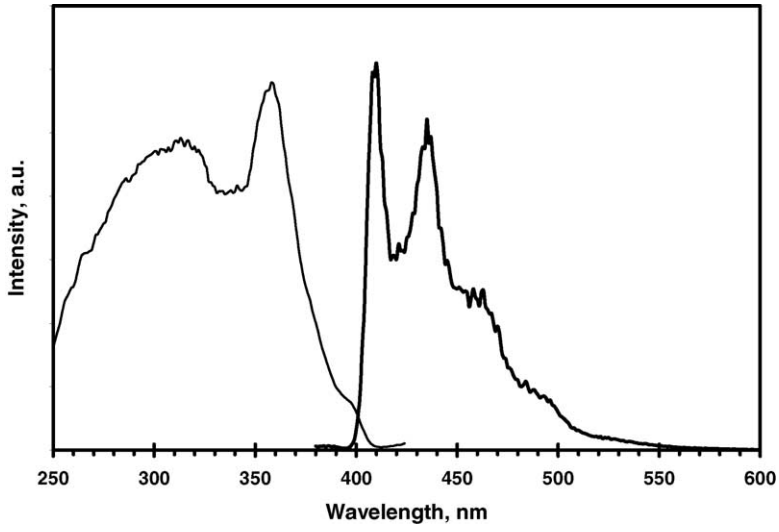

Fig. 2. Emission (right) and corrected excitation (left) spectra of a crystalline sample of **1** at 77 K.

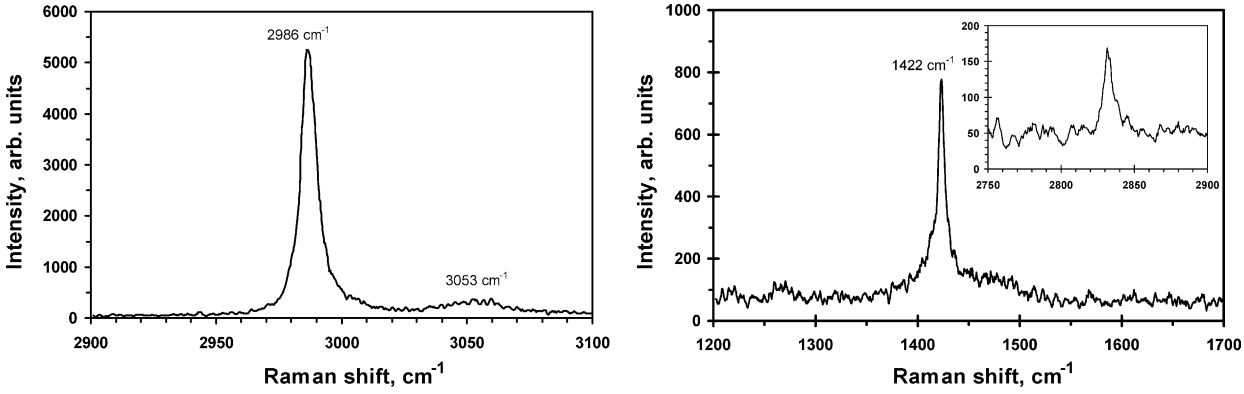

Fig. 3. Raman spectrum of a solution of **1** in CH_2Cl_2 at ambient temperature.

shows a 1:1 sandwich adducts, **1**·$C_{10}F_8$, with a supramolecular infinite-chain structure. The packing of the molecules in a $\{\mathbf{1}\cdot C_{10}F_8\}_\infty$ chain is shown in Fig. 4. Similar 1:1 stacks form between **1** and another perfluorinated aromatic molecule, C_6F_6 (vide infra). Given the nucleophilic character of **1** and the known electrophilic character of the Lewis acids C_8F_{10} and C_6F_6, electrostatic interactions are expected to be the dominant forces that stabilize the supramolecular structure of both $\{\mathbf{1}\cdot C_{10}F_8\}_\infty$ and $\{\mathbf{1}\cdot C_6F_6\}_\infty$ π acid–base stacks. The distance between the centroid of $C_{10}F_8$ to the centroid of **1** is 3.509 Å compared to the slightly longer distance of 3.565 Å in **1**·C_6F_6. The Au···Au intramolecular interactions in **1** (3.224, 3.288 and 3.299 Å) become longer upon adduct formation in **1**·$C_{10}F_8$ (3.279, 3.280, 3.337 Å). There is no significant change in the distances in the fluorinated naphthalene rings upon adduct formation. This is consistent with a recent report by Schafer and co-workers [32] in which the authors have shown that the neutral and anionic forms of $C_{10}F_8$ both possess a D_{2h} symmetry and the electron affinity of the neutral species is 1.01 eV compared to 0.69 eV for hexafluorobenzene. The larger electron affinity of $C_{10}F_8$ than that of C_6F_6 explains the shorter interplanar separation in **1**·$C_{10}F_8$ compared to **1**·C_6F_6.

The **1**·$C_{10}F_8$ solid adduct exhibits a yellow emission band that is bright even at ambient temperature. Fig. 5 shows the emission spectra of crystals of **1**·$C_{10}F_8$ in comparison with the solid uncomplexed $C_{10}F_8$ aromatic molecule. A structured profile is observed for **1**·$C_{10}F_8$ with a better resolution obtained upon cooling to 77 K. The profile is essentially the same as that of crystals of uncomplexed octafluoronaphthalene but there is a slight red shift. At ambient temperature, the yellow organic-centered luminescence is very bright for **1**·$C_{10}F_8$ but undetectable for solid octafluoronaphthalene.

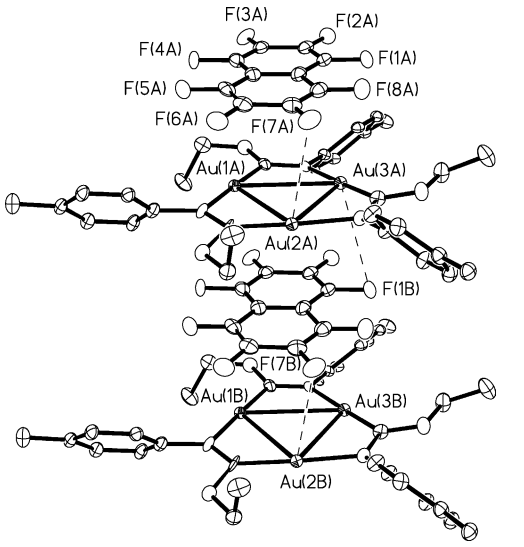

Fig. 4. Thermal ellipsoid drawing of the stacked octafluoronaphthalene with **1**.

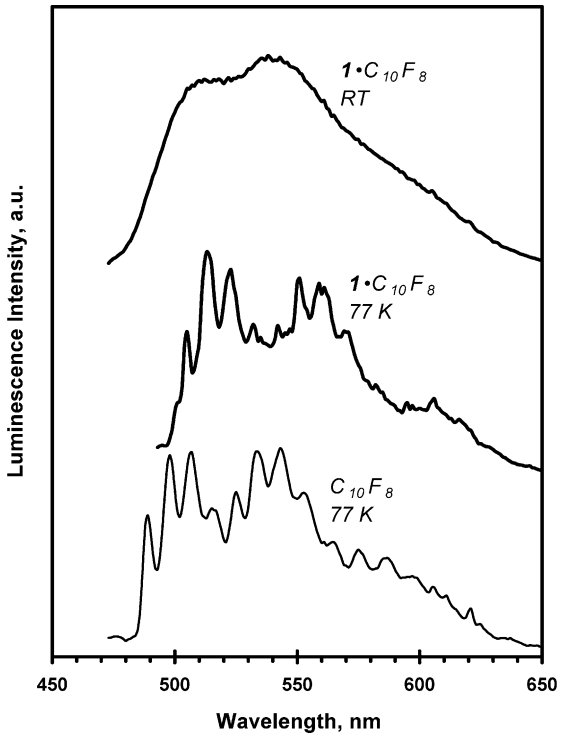

Fig. 5. Emission spectra of single crystals of the **1**·$C_{10}F_8$ stacked adduct and solid $C_{10}F_8$. No luminescence was detected at room temperature from solid $C_{10}F_8$.

Lifetime measurements show that the yellow luminescence of **1**·$C_{10}F_8$ is phosphorescence. The decay curve at 550 nm shows a single exponential fit with $\tau = 3.57 \pm 0.07$ ms. The magnitude of the lifetime did not change significantly with variations in either the laser excitation wavelength or the monitored emission wavelength.

The structured profile, energy, and lifetime of the yellow emission of the **1**·$C_{10}F_8$ adduct indicate that the emission can be assigned to monomer phosphorescence of the octafluoronaphthalene, for which the energy of the $T_1 \rightarrow S_0$ radiative transition is red shifted only slightly. The 3.6 ms lifetime of the yellow emission of **1**·$C_{10}F_8$ is two orders of magnitude shorter than the lifetime of the octafluoronaphthalene phosphorescence, which was reported to be in the range of 0.25–0.38 s in frozen glasses [33–35]. The brightness of the yellow phosphorescence at room temperature for the **1**·$C_{10}F_8$ solid adduct along with the great reduction in the lifetime compared to free octafluoronaphthalene are indicative of a strong gold heavy-atom effect. The slight red shift in the emission energy of **1**·$C_{10}F_8$ is also a known consequence of the heavy-atom effect [33,35]. The interactions between **1** and octafluoronaphthalene are secondary π interactions, as evidenced by the relatively long crystallographic distances between the planes of the two components (~3.5 Å between the centroids). The energies of such interactions have been estimated to be in the range of only 1–2 kcal/mol in similar systems [36,37]. Hence, one can consider the heavy-atom effect seen here for the **1**·$C_{10}F_8$ adduct to be more comparable to the external heavy-atom effect known for organic compounds when a heavy atom is present in the luminophore environment (e.g., in the solvent, host matrix, or "through space" interactions within the molecule), as opposed to the internal heavy-atom effect where a heavy atom is involved in a direct covalent bonding to the luminophore [38–42]. The external heavy-atom effect in organic compounds usually leads to a modest decrease in phosphorescence lifetimes while this decrease is much more significant in the case of the internal heavy-atom effect. For example, substituting naphthalene ($\tau^P = 2.6$ s) with Br and norborane-Br reduces the lifetime to 0.02 and 0.11 s due to internal and external heavy-atom effects, respectively [38,39]. The reduction in phosphorescence lifetime seen for **1**·$C_{10}F_8$ to ms levels due to an external heavy-atom effect of gold is much more significant than the common reduction in τ^P due to external heavy-atom effects and is more comparable to the reduction in τ^P due to internal heavy-atom effects. The spin–orbit coupling "ζ" parameter for the 5d orbital of Au(I) is 5100 cm^{-1} [43], comparable to the ζ values for the Br and I atoms of 2460 and 5700 cm^{-1}, respectively [39,44]. The internal heavy-atom effect in α-iodonaphthalene leads to $\tau^P = 2$ ms [39]. Meanwhile, lifetime data recently communicated by Omary and Gabbaï show τ^P values on the order of 10^{-1} to 10^0 ms for several 1:1 adducts of electron-rich aromatic hydrocarbons (naphthalene; biphenyl; pyrene) with the macrocyclic Lewis acid μ-(*o*-C_6F_4)$_3$$Hg_3$ [24]. Therefore, it is reasonable to conclude that secondary π interactions of aromatic luminophores with trinuclear complexes of $5d^{10}$ heavy metal ions lead to an unusually strong external heavy-atom effect that is comparable to the internal heavy-atom effect in organic compounds. The long-range ordering of the acid–base stacks in which each organic triplet emitter is surrounded by six heavy metal atoms is likely the major contributing factor to the unusually strong external heavy-atom effect seen here. This effect, however, is smaller than the internal effect in which metals are involved in coordinate covalent bonds with the organic moiety, wherein τ^P values of 10^1–10^2 μs are common for ligand-centered emissions in $5d^{10}$ complexes [45] and even in lighter $3d^{10}$ and $4d^{10}$ complexes [46]. The phosphorescence lifetimes are even shorter for metal-centered emissions, wherein τ^P values of a few microseconds and even 10^2 ns are quite common, e.g., for Au(I) complexes that show gold-centered emissions [47].

In order to gain insight into the photophysical processes that lead to the enhanced phosphorescence in **1**·$C_{10}F_8$, absorption, diffuse–reflectance, and luminescence excitation spectra were obtained. Fig. 6 shows the diffuse reflectance spectrum of the solid adduct **1**·$C_{10}F_8$. Because the adduct stacks in a 1:1 manner, the diffuse reflectance data are compared with the absorption spectra for dilute solutions of **1** and of $C_{10}F_8$, which represent monomers of these species. Fig. 6 shows the **1**·$C_{10}F_8$ adduct exhibits not only absorptions characteristic of its two monomer components, but also new red-shifted features (designated by arrows) that extend the absorption edge of the adduct to approach the visible region. Luminescence excitation spectra suggest that these new absorptions represent the major excitation route that leads to the yellow luminescence of **1**·$C_{10}F_8$. Fig. 7 shows that distinct luminescence excitation peaks appear near 335 and 360 nm for **1**·$C_{10}F_8$, which correspond to the red-shifted diffuse–reflectance features. The fact that these new features become much more clearly discernible in the luminescence excitation spectrum than they were in the diffuse reflectance spectrum indicates the central role played by their corresponding transitions in the excitation route of **1**·$C_{10}F_8$. For

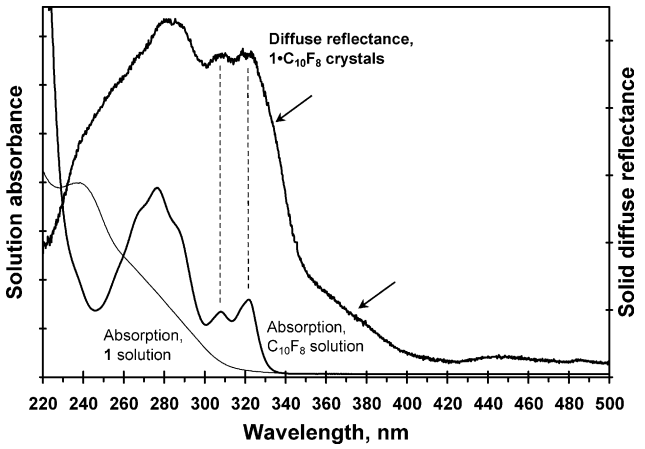

Fig. 6. Solid-state diffuse reflectance spectrum of the **1**·$C_{10}F_8$ stacked adduct in comparison to its free molecular components, represented by dilute solutions of **1** and octafluoronaphthalene in acetonitrile.

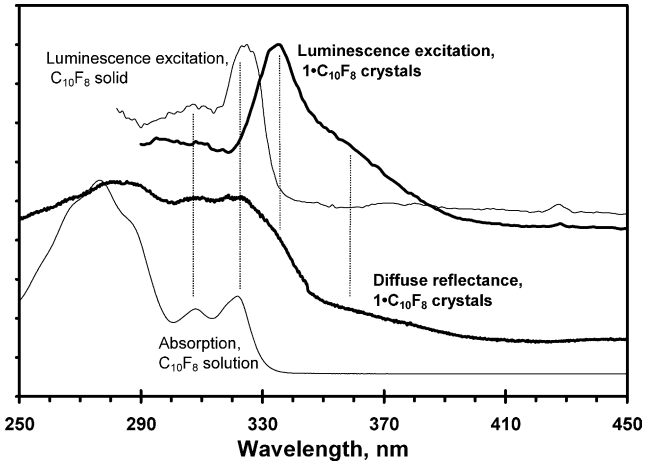

Fig. 7. Overlay of various electronic spectra of **1**·$C_{10}F_8$ and free $C_{10}F_8$ for purposes of comparison.

comparison, Fig. 7 also shows the luminescence excitation spectrum of $C_{10}F_8$ alone, which exhibits luminescence excitation peaks at shorter wavelengths and correspond to the monomer absorption peaks in the absorption spectrum of dilute solutions of $C_{10}F_8$.

We assign the diffuse reflectance/excitation peaks at ~335 and 360 nm for **1**·$C_{10}F_8$ to charge-transfer transitions in the ground state adduct. The trinuclear Au(I) complex **1** is strongly nucleophilic (Section 2.1), so it acts as a π base and donates electron density to the π acid $C_{10}F_8$. The resulting charge-transfer adduct exhibits characteristic absorptions that are red-shifted from the absorptions of its individual components. Kisch et al. suggested that donor-to-acceptor charge-transfer bands should appear in the diffuse–reflectance spectra of 1:1 donor:acceptor inorganic:organic ionic solid stacks [48]. Also, previous work by us (vide infra; Section 3.3) [8] and by Balch and co-workers [21b] showed that charge-transfer absorption bands in the visible and near IR regions arise in *neutral* adducts that form upon interaction of trinuclear Au(I) complexes with organic acceptors such as TCNQ and nitro-substituted fluorenones. No luminescence data were reported in these previous reports, but they support the charge-transfer assignment of the lowest-energy diffuse–reflectance/excitation peaks of **1**·$C_{10}F_8$. Although the mechanism of the external heavy-atom effect of organic luminophores has been subject to numerous interpretations [49] and there seems to be lack of consensus on its origin, it has been suggested that charge transfer might play a role in the external heavy-atom effect. Evidence to this effect has been gathered, typically by analysis of the emission data for rigid glasses at cryogenic temperatures for a number of related luminophores that contain one or more heavy-atoms (usually halogens), or by theoretical studies [49]. But, to our knowledge, distinct peaks due to the suggested charge-transfer process in the ground-state adduct, like those shown in Figs. 6 and 7, have not been reported for conventional organic luminophores that exhibit phosphorescence due to an external heavy-atom effect.

The conventional heavy-atom effect in organic molecules usually invokes a phosphorescence route that entails simply the enhancement of the S_1–T_1 intersystem crossing of the organic compound following direct absorption from S_0 to either S_1 or a higher singlet (e.g., S_2) that then relaxes to S_1 via internal conversion [38,39]. In contrast, the spectral data for the **1**·$C_{10}F_8$ adduct here suggest a different excitation route for the phosphorescence, as depicted in Fig. 8. Absorption occurs directly to the resulting charge-transfer states in the **1**·$C_{10}F_8$ adduct. The significantly lower intensity of the lowest-energy feature near 360 nm in the diffuse reflectance and excitation spectra of the adduct suggests that it represents a triplet charge transfer state (^{3}CT) while the higher energy feature near 335 nm is assigned to a singlet charge transfer state (^{1}CT). Fortunately, these charge transfer states lie higher in energy than the energy of the T_1 state of the organic component such that the latter state will not be depopulated as a result of the charge transfer process. Thus, the lowest-energy emitting state in the adduct remains as the T_1 state with little perturbation of its original energy in the organic component alone. The spectral data suggest that the S_1 state of $C_{10}F_8$ is not involved in the charge transfer process because vibronic features corresponding to this state remain essentially unperturbed in the spectrum of the binary adduct (see the dashed lines in Fig. 6). Hence, we illustrate in Fig. 8 that the ^{3}CT and ^{1}CT states arise from the molecular orbital interaction of the T_2 and S_2 states of $C_{10}F_8$ with suitable frontier orbitals in **1** while both the S_1 and T_1 states of $C_{10}F_8$ remain non-bonding in the **1**·$C_{10}F_8$ adduct. The luminescence excitation spectrum that monitors the yellow phosphorescence (Fig. 7) suggests that the charge transfer process represents the major low-energy excitation route while excitation peaks due to direct absorption to the triplet are absent (e.g., $S_0 \rightarrow T_1$ absorptions for naphthalenes lie between 400 and 500 nm) [39].

3.2. Hexafluorobenzene adduct

Unlike the **1**·$C_{10}F_8$ adduct, the **1**·C_6F_6 adduct does not exhibit detectable phosphorescence from the T_1 state of C_6F_6

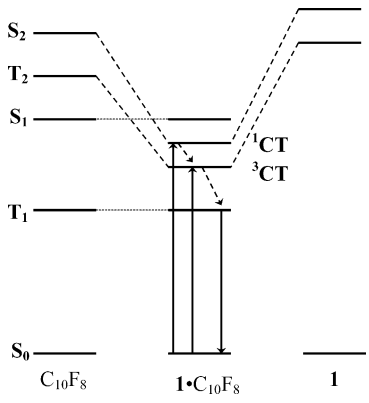

Fig. 8. Proposed energy level diagram showing the interaction between the excited states of **1** and $C_{10}F_8$ to form the charge transfer (CT) states in the **1**·$C_{10}F_8$ adduct.

on complexation with **1**. A reasonable explanation may lie in the fact that previous experimental data in the organic literature suggest that perfluorination leads to an internal heavy-atom effect for the octafluoronaphthalene ring but not for the hexafluorobenzene ring (for further details, see refs. [34,50]). The **1**·C_6F_6 solid adduct is actually not luminescent at all even at cryogenic temperatures. Because **1** exhibits intermolecular Au–Au interactions between adjacent trimers (Section 2.1) and exhibits blue phosphorescence (Section 2.2) while both these interactions are absent in the non-luminescent 1:1 stacks of the **1**·C_6F_6 solid adduct, we hypothesized that the presence of luminescence in **1** and its absence in **1**·C_6F_6 are related to the presence or absence of intermolecular Au–Au interactions between adjacent trimers. This hypothesis was substantiated by our observation that, when **1**·C_6F_6 is immersed in a solvent that does not dissolve **1**, e.g., Et_2O, the compound loses its crystallinity and the resulting powder exhibits the same blue photoluminescence characteristic of **1**, indicating that C_6F_6 is liberated from **1**·C_6F_6. In contrast, when solid **1** is suspended in C_6F_6, its blue luminescence starts to quench with time. These observations prompted a study of the interaction of these complexes with vapors of organic compounds. Fig. 9 shows a representative example. A solid sample of **1** was placed at a fixed position in a closed chamber and its luminescence spectra were acquired as a function of time in the presence of C_6F_6 vapors. The vapors were produced as a result of the vapor pressure at ambient temperature and pressure of a liquid sample of neat C_6F_6 in a small beaker that is placed at the bottom of the closed chamber. The quenching of the luminescence of **1** was first detected after only several minutes and continued gradually until the next day (Fig. 9). A control experiment in the absence of C_6F_6 vapors was carried out and showed no quenching in the luminescence of **1** with time.

The evidence we have gathered thus far suggests that, **1**·C_6F_6 dissociates in solution into its component trinuclear Au(I) compound and organic Lewis acid. The electronic absorption spectra for solutions of **1**·C_6F_6 show the same absorption peaks as those for **1** and C_6F_6. The ^{19}F NMR spectra for even nearly saturated solutions of **1**·C_6F_6 in $CDCl_3$ show one peak at the same chemical shift (−168 ppm) as that observed for C_6F_6 alone in $CDCl_3$.

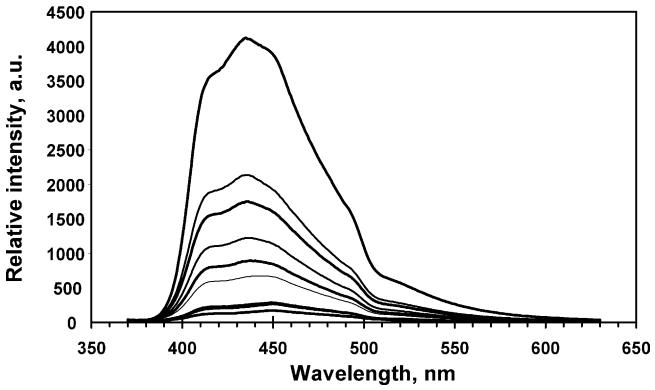

Fig. 9. Emission spectra of **1** vs. exposure time to C_6F_6 vapor at ambient temperature and pressure. The exposure time was (top-to-bottom) 0, 51, 65, 98, 148, 208, 1322, 1439, and 1462 min, respectively [8].

3.3. Tetracyanoquinodimethane adduct

Reaction of a saturated solution of 7,7,8,8-tetracyanoquinodimethane with a sample of **2** added dropwise results in an instant dramatic color change from light yellow to intense green. Crystallization produced dark crystals whose structure showed infinite 2:1 stacks, $\{[\mathbf{2}]_2\cdot TCNQ\}_\infty$, as shown in Fig. 10 [8]. The TCNQ molecule is sandwiched between two units of **2** from each side, in a face-to-face manner so that a molecule of the **2**·TCNQ adduct is best represented by the formula (π-**2**)(μ-π-TCNQ)(π-**2**). The cyanide groups are clearly not coordinated to the gold atoms; hence, π acid–base interactions are favored to σ coordination of TCNQ to the trinuclear **2** despite the strong σ donation ability of TCNQ and the low coordination number, 2, for the Au atoms in **2**. Although the distance between the centroid of TCNQ to the centroid of the Au_3 unit is very long, 3.964 Å, consistent with the aforementioned nature of such secondary π

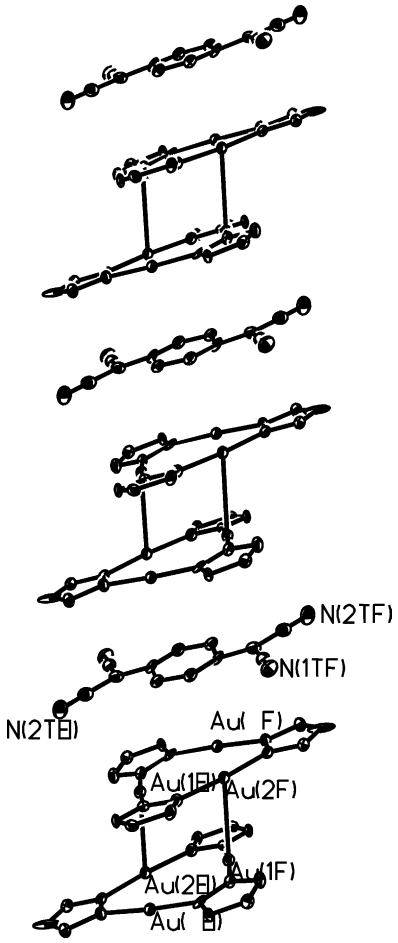

Fig. 10. Crystal structure of the **2**·TCNQ adduct showing a view of the columnar structure formed by the repeat unit. The benzyl groups are omitted for clarity [8].

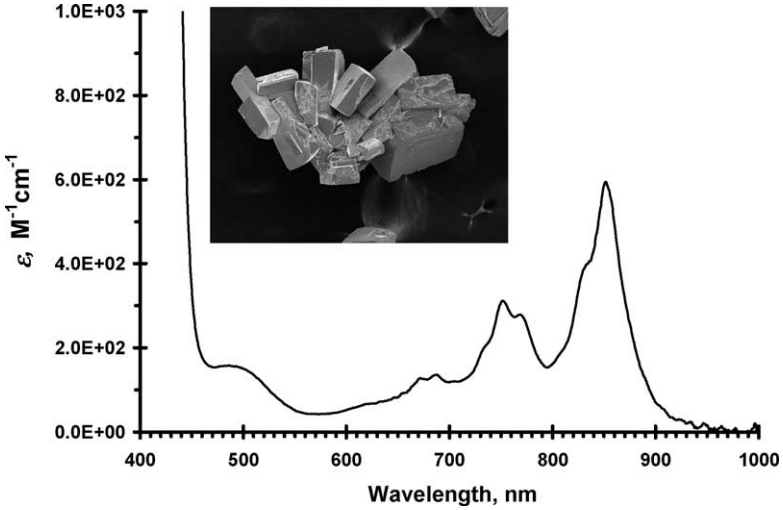

Fig. 11. Visible absorption spectrum of **2** TCNQ in CH_2Cl_2 at room temperature. The insert shows the SEM image of the crystals taken without a conductive film coating [8].

interactions, dramatic changes in the physical and electronic properties take place as a result of these interactions. Multiple evidence has been collected to suggest the presence of partial charge delocalization in the $\{[\mathbf{2}]_2{\cdot}TCNQ\}_\infty$ stacks. First, the intermolecular Au–Au distances were shortened significantly; they were even shorter than the intramolecular Au–Au distances in which ligand assistance plays a role. This may be ascribable to charge-transfer from the electron-rich Au center to the electron acceptor TCNQ; a partial oxidation of the Au(I) atoms leads to a shortening of Au–Au distances. In the limiting case, upon oxidation to Au(II), a gold–gold single bond forms [51]. Second, the intense dark green color of the adduct, in contrast to the colorless crystals of **1** and the pale brown crystals of TCNQ, may be an indication of charge transfer; similar color changes were used as evidence of charge transfer in a previous study by Balch for adducts of trinuclear Au(I) carbeniate complexes with nitro-9-fluorenones [21b]. Likewise, Perutz and co-workers reported a red charge-transfer complex that forms as a result of a reaction between bis(η^6-benzene)chromium and hexafluorobenzene [52]. There is more relevance for the latter study with the **2**·TCNQ adduct discussed here than with the **1**·C_6F_6 adduct discussed in the previous section. The charge transfer adduct forming between **2** and TCNQ possibly remains intact in solution because the solutions of the adduct are deeply colored. Fig. 11 shows the absorption spectrum of the adduct in a CH_2Cl_2 solution. The spectrum shows visible and NIR absorptions. The absorption peak near 500 nm may be due to charge transfer because **2** and TCNQ alone absorb below 400 nm. Both neutral TCNQ and $TCNQ^-$ absorb in the NIR region with stronger absorptions for the anionic form ($\varepsilon_{max} = 43{,}300\ M^{-1}\ cm^{-1}$); partially reduced TCNQ will likely exhibit similar NIR absorptions. The spectrum in Fig. 11 appears to show a small amount of anionic $TCNQ^-$ but it is hard to distinguish absorptions due to the partially reduced TCNQ that are expected to be the dominant TCNQ species in solution from absorptions due to the neutral form and the fully reduced anionic $TCNQ^-$ form. Unfortunately these spectral observations are not definitive regarding the actual species present. Third, a scanning-electron microscope (SEM) image for crystals of **2**·TCNQ is shown in the inset of Fig. 11. The observation of a clear SEM image for crystals of **2**·TCNQ that were not coated with a conducting material suggests that these crystals are non-insulators, because the charge from the electron beam accumulates on the surface of insulating materials, which precludes the observation of a clear SEM image for an insulator [53]. Conducting or semiconducting materials, on the other hand, can diffuse the charge and, thus, allow for the observation of a clear SEM image. We have attempted to carry out preliminary resistivity measurements for a large crystal of **2**·TCNQ that we were able to grow from a saturated CH_2Cl_2 solution containing **1** and TCNQ at 4 °C. However, the resistivity of the crystals at ambient temperature was too high to be measured with the setup we had access to, which can only measure resistivities for conducting materials. The apparent optical band gap of **2**·TCNQ (the absorption edge) is about 1.4 eV, which is within the band gap region for semiconductors, not conductors.

4. Conclusions

Although metal centers are usually electrophilic, we have shown via solid evidence based on X-ray crystallography, electronic absorption and luminescence spectroscopy, and quantum mechanical calculations that the trinuclear Au(I) complexes studied herein are strong π bases. Their nucleophilic nature allows them to form acid–base adducts with a variety of organic and inorganic electrophiles. The photophysical properties vary in the different adducts depending on the interacting electrophile. These included the sensitization of the phosphorescence of the aromatic electrophiles via

a gold heavy-atom effect, the quenching of the Au-centered emission by disrupting the Au–Au intermolecular interactions by the organic electrophile, the formation of intense charge transfer absorptions in the visible and NIR regions, and metal-centered thermochromic luminescence bands delocalized along the stacking M–M chain axis when the electrophile contains a heavy metal. These fascinating photophysical properties promise a great potential for the utilization of such supramolecular acid–base stacks in a variety of optoelectronic applications that include molecular LEDs, selective optical sensing of hazardous small molecules and heavy metals, optical telecommunication devices, and solar cell dyes.

Acknowledgments

The financial support of this project has been provided by the Robert A. Welch Foundation of Houston, TX, to J.P.F. and M.A.O., a National Science Foundation CAREER award to M.A.O. (CHE-0349313), and an Advanced Technology Program grant from the Texas Higher Education Coordinating Board to M.A.O. We also thank Professor Alfredo Burini of the University of Camerino for initiating collaborative studies with the trinuclear Au(I) complexes.

References

[1] G.N. Lewis, J. Franklin Inst. 226 (1938) 293;
G.N. Lewis, Valence and the Structure of Atoms and Molecules, Chemical Catalog Co., New York, 1978, p. 141.
[2] (a) C.K. Ingold, J. Chem. Soc. (1933) 1120;
C.K. Ingold, Chem. Rev. 15 (1934) 225;
C.K. Ingold, Structure and Mechanism in Organic Chemistry, Cornell, Ithaca, New York, 1953 (Chapter V);
(b) R. Robinson, Outline of an Electrochemical (Electronic) Theory of the Course of Organic Reactions, Institute of Chemistry, London, 1932, p. 12.
[3] W.B. Jensen, The Lewis Acid–base Concepts, Wiley, New York, 1980.
[4] A. Burini, R. Bravi, J.P. Fackler Jr., R. Galassi, T.A. Grant, M.A. Omary, B.R. Peitroni, R.J. Staples, Inorg. Chem. 39 (2000) 3158.
[5] A. Burini, J.P. Fackler Jr., R. Galassi, B.R. Pietroni, R.J. Staples, Chem. Commun. (1998) 95.
[6] A. Burini, J.P. Fackler Jr., R. Galassi, A. Macchioni, M.A. Omary, M.A. Rawashdeh-Omary, B.R. Pietroni, S. Sabatini, C. Zuccaccia, J. Am. Chem. Soc. 124 (2002) 4570.
[7] A. Burini, J.P. Fackler Jr., R. Galassi, T.A. Grant, M.A. Omary, M.A. Rawashdeh-Omary, B.R. Pietroni, R.J. Staples, J. Am. Chem. Soc. 122 (2000) 11264.
[8] M.A. Rawashdeh-Omary, M.A. Omary, J.P. Fackler Jr., R. Galassi, B.R. Pietroni, A. Burini, J. Am. Chem. Soc. 123 (2001) 9689.
[9] A. Burini, A.A. Mohamed, J.P. Fackler Jr., Comments Inorg. Chem. 24 (2003) 253.
[10] J.K. Bera, K.R. Dunbar, Angew. Chem. Int. Ed. 41 (2002) 4453.
[11] R. Hoffmann, Angew. Chem., Int. Ed. Engl. 26 (1987) 846.
[12] J.S. Miller (Ed.), Extended Linear-Chain Compounds, vols. 1–3, Plenum Press, New York, 1982.
[13] Y. Kunugi, K.R. Mann, L.L. Miller, C.L. Exstrom, J. Am. Chem. Soc. 120 (1998) 589.
[14] M.A. Mansour, W.B. Connick, R.J. Lachicotte, H.J. Gysling, R. Eisenberg, J. Am. Chem. Soc. 120 (1998) 1329.
[15] (a) E.J. Fernandez, J.M. Lopez-de-Luzuriaga, M. Monge, M.E. Olmos, J. Perez, A. Laguna, A.A. Mohamed, J.P. Fackler Jr., J. Am. Chem. Soc. 125 (2003) 2022;
(b) E.J. Fernández, J.M. López-de-Luzuriaga, M. Monge, M. Montiel, M.E. Olmos, J. Pérez, A. Laguna, F. Mendizabal, A.A. Mohamed, J.P. Fackler Jr., Inorg. Chem. 43 (2004) 3573–3581.
[16] W.R. Caseri, H.D. Chanzy, K. Feldman, M. Fontana, P. Smith, T.A. Tervoort, J.G.P. Goossens, E.W. Meijer, A.P.H.J. Schenning, I.P. Dolbyna, M.G. Debije, M.P. de Haas, J.M. Warman, A.M. van de Craats, R.H. Friend, H. Sirringhaus, N. Stutzmann, Adv. Mater. 15 (2003) 125.
[17] (a) H. Tanaka, Y. Okano, H. Kobayashi, W. Suzuki, A. Kobayashi, Science 291 (2001) 285;
(b) F. Bigoli, P. Deplano, M.L. Mercuri, M.A. Pellinghelli, L. Pilia, G. Pintus, A. Serpe, E.F. Trogu, Inorg. Chem. 41 (2002) 5241;
(c) N. Robertson, L. Cronin, Coord. Chem. Rev. 227 (2002) 93;
(d) H. Kisch, B. Eisen, R. Dinnebier, K. Shankland, W.I.F. David, F. Knoch, Chem. Eur. J. 7 (2001) 738.
[18] B.W. Smucker, J.M. Hudson, M.A. Omary, K.R. Dunbar, Inorg. Chem. 42 (2003) 4714.
[19] M.A. Rawashdeh-Omary, M.A. Omary, J.P. Fackler Jr., Inorg. Chim. Acta 334 (2002) 376.
[20] M. Stender, R.L. White-Morris, M.M. Olmstead, A.L. Balch, Inorg. Chem. 42 (2003) 4504.
[21] (a) J.C. Vickery, M.M. Olmstead, E.Y. Fung, A.L. Balch, Angew. Chem. Int. Ed. Engl. 36 (1997) 1179;
(b) M.M. Olmstead, F. Jiang, S. Attar, A.L. Balch, J. Am. Chem. Soc. 123 (2001) 3260;
(c) A. Hayashi, M.M. Olmstead, S. Attar, A.L. Balch, J. Am. Chem. Soc. 124 (2002) 5791.
[22] G. Yang, R.G. Raptis, Inorg. Chem. 42 (2003) 261.
[23] M.R. Haneline, M. Tsunoda, F.P. Gabbaï, J. Am. Chem. Soc. 124 (2002) 3737.
[24] M.A. Omary, R.M. Kassab, M.R. Haneline, O. Elbjeirami, F.P. Gabbaï, Inorg. Chem. 42 (2003) 2176.
[25] H.V.R. Dias, H.V.K. Diyabalanage, M.A. Rawashdeh-Omary, M.A. Franzman, M.A. Omary, J. Am. Chem. Soc. 125 (2003) 12072.
[26] A. Tiripicchio, M.T. Camellini, G. Minghetti, J. Organomet. Chem. 171 (1979) 399.
[27] M.A. Rawashdeh-Omary, M.A. Omary, L. Daniels, J.P. Fackler Jr., in preparation.
[28] H. Schmidbaur (Ed.), Gold: Progress in the Chemistry, Biochemistry and Technology, John Wiley & Sons, Chester, England, 1999.
[29] S. Mecozzi, A.P. West, D.A. Dougherty, Proc. Natl. Acad. Sci. U.S.A. 93 (1996) 10566, and references therein.
[30] M.A. Omary, J. Park, M.A. Rawashdeh-Omary, S.W. North, J.P. Fackler Jr., in preparation.
[31] A.A. Mohamed, M.A. Rawashdeh-Omary, M.A. Omary, J.P. Fackler Jr., in preparation.
[32] Y. Xie, H.F. Schaefer, F.A. Cotton, Chem. Commun. (2003) 102.
[33] J.C. Miller, J.S. Meek, S.J. Strickler, J. Am. Chem. Soc. 99 (1977) 8175, and references therein.
[34] H.B. Rosenberg, S.D. Carson, J. Phys. Chem. 72 (1968) 3531.
[35] V.L. Ermolaev, K.J. Svitashev, Opt. Spektrosk. 7 (1959) 664.
[36] E.F. Kiefer, W.L. Waters, D.A. Carlson, J. Am. Chem. Soc. 90 (1968) 5127.
[37] W. Kitching, G.M. Drew, V. Alberts, Organometallics 1 (1982) 331.
[38] N.J. Turro, Modern Molecular Photochemistry, University Science Books, Sausalito, CA, 1991.
[39] S.P. McGlynn, T. Azumi, M. Kinoshita, Molecular Spectroscopy of the Triplet State, Prentice-Hall, Englewood Cliffs, New Jersey, 1969.
[40] D.S. McClure, N.W. Blake, P.L. Hanst, J. Chem. Phys. 22 (1954) 255.
[41] V.L. Ermolaev, K.J. Svitashev, Opt. Spektrosk. 7 (1959) 399.
[42] M. Kasha, J. Chem. Phys. 20 (1952) 71.

[43] J.S. Griffith, Theory of Transition Metal Ions, Cambridge University Press, Cambridge, 1964.
[44] J. Friedrich, F. Metz, F. Dörr, Mol. Phys. 30 (1975) 289.
[45] H-Y. Chao, W. Lu, Y. Li, M.C.W. Chan, C.-M. Che, K.-K. Cheung, N. Zhu, J. Am. Chem. Soc. 124 (2002) 14696.
[46] M.A. Omary, M.A. Rawashdeh-Omary, H.V.K. Diyabalanage, H.V.R. Dias, Inorg. Chem. 42 (2003) 8612.
[47] For reviews, see;
(a) J.M. Forward, J.P. Fackler Jr., Z. Assefa, in: D.M. Roundhill, J.P. Fackler Jr. (Eds.), Optoelectronic Properties of Inorganic Compounds, Plenum, New York, 1999 (Chapter 6);
(b) V.W.-W. Yam, K.K. Lo, Chem. Soc. Rev. 28 (1999) 323.
[48] (a) H. Kisch, B. Eisen, R. Dinnebier, K. Shankland, W.I.F. David, F. Knoch, Chem. Eur. J. 7 (2001) 738;
(b) H. Kisch, Comments Inorg. Chem. 16 (1994) 113.
[49] A comprehensive citation of papers about the mechanism of the external heavy-atom effect is inappropriate but representative examples include [42] and the following with references therein;
(a) T. Azumi, Chem. Phys. Lett. 19 (1973) 580;
(b) A.K. Chandra, N.J. Turro, A.L. Lyons Jr., P. Stone, J. Am. Chem. Soc. 100 (1978) 4964;
(c) B.F. Minaev, S. Knuts, H. Ågren, Chem. Phys. Lett. 181 (1994) 15;
(d) N. Chattopadhyay, C. Serpa, M.M. Pereira, J. Seixas de Melo, L.G. Arnaut, S.J. Formosinho, J. Phys. Chem. A 105 (2001) 10025;
(e) I.R. Gould, J.A. Boiani, E.B. Gaillard, J.L. Goodman, S. Farid, J. Phys. Chem. A 107 (2003) 3515.
[50] D. Phillips, J. Chem. Phys. 46 (1967) 4679.
[51] For example, see;
(a) T.F. Carlson, J.P. Fackler Jr., J. Organomet. Chem. 596 (2000) 237;
(b) V.W.W. Yam, S.W.K. Choi, K.K. Cheung, Chem. Commun. (1996) 1173;
(c) J.P. Fackler Jr., Inorg. Chem. (2002) 6959;
(d) M.D. Irwin, H.E. Abdou, A.A. Mohamed, J.P. Fackler Jr., Chem. Commun. (2003) 2882–2883.
[52] C.J. Aspley, C. Boxwell, M.L. Buil, C.L. Higgitt, C. Longb, R.N. Perutz, Chem. Commun. (1999) 1027.
[53] J.I. Goldstein, D.E. Newbury, P. Echlin, D.C. Joy, A.D. Romig Jr., C.E. Lyman, C. Fiori, E. Lifshin, Scanning Electron Microscopy and X-ray Microanalysis: A Text for Biologists, Materials Scientists, and Geologists, Plenum Press, New York, 1992.